R. & M. No. 2651
(11,645)
A.R.C. Technical Report

MINISTRY OF SUPPLY

AERONAUTICAL RESEARCH COUNCIL
REPORTS AND MEMORANDA

Concerning the Annular Air Intake in Supersonic Flight

By

I. M. DAVIDSON and L. E. UMNEY

LONDON : HER MAJESTY'S STATIONERY OFFICE

1952

SIX SHILLINGS NET

Concerning the Annular Air Intake in Supersonic Flight

By

I. M. DAVIDSON and L. E. UMNEY

COMMUNICATED BY THE PRINCIPAL DIRECTOR OF SCIENTIFIC RESEARCH (AIR), MINISTRY OF SUPPLY

Reports and Memoranda No. 2651*
August, 1947

Summary.—The stability of an annular air intake at a Mach number of 1·4 and with Reynolds numbers of about $1{\cdot}5\times10^6$ is considered in detail and a method is described whereby the experimental results might be extrapolated for preliminary full-scale design purposes. This extrapolation has yet to be checked experimentally, but suggests that a typical aircraft intake would have an overall isentropic efficiency of about 85 per cent. The results also indicate that both the stability and the efficiency of an intake could be improved by controlling the boundary layer on its nacelle, and as an alternative to boundary-layer suction a device which is described as a segregation ring is suggested. This, it appears, might raise the efficiency by some 2 or 3 per cent.

1. *Introduction.*—At high flight speeds intakes of the annular or letterbox variety are especially desirable for the considerable advantages made possible by their adoption. Amongst these are structural simplicity, reduced fuselage form and frictional drag, a good field of view for the pilot and the possibility of concentrating the useful load in the nose of the machine.

However, from the inconclusive results of some previous tests[1,2] it seemed probable that these advantages could be realised only at the expense of considerable intake loss and with the risk of incurring a catastrophic aerodynamic instability.

The experimental programme culminating in this note was designed only to investigate these phenomena in models but it is believed that the results obtained might, with care, be extrapolated for full-scale preliminary design purposes.

2. *Experimental Equipment and Procedure.*—The apparatus consisted substantially of a 6-in. diameter open-jet wind-tunnel, a metering nacelle to which various models could be adapted and a striation system based on a spherical mirror of diameter 10 in. and radius of curvature 96 in. A general arrangement is shown in Fig. 1, the metering nacelle in Fig. 2 and the optical system in Fig. 3.

As the tunnel air, supplied at about four atmospheres absolute and 470 deg K by a four-stage centrifugal compressor, was used without cooling no undesirable condensation effects could have occurred. The programme involved the use of only a single effuser of Mach number 1·4 and, although the velocity distribution in the working section was rather poor, it was considered adequate for the purposes of the investigation.

In all, six different intakes were tested and, being designated respectively models A, B, C, D, E and F, these are described by Fig. 4. For the subsequent diffusion within the metering nacelle two different types of ducting system were used and examples of these are given in Fig. 5.

*N.G.T.E. Report R.16—received 30th July, 1948.

To avoid serious erosion different intake leading edge thicknesses were used on successive models, but all were between 0·005 in. and 0·015 in. and in no case was the edge rounded. However, this fact should not materially have influenced the results, for edges as badly eroded as that illustrated in Fig. 6 produced no measurable increment in the intake loss.

During the initial tests, complete traverses were performed within the nacelle for each setting of the exit throttle, and a check was thus obtained on both the mass flow and the intake efficiency. However, it was discovered that, because of the small dynamic head in the nacelle, the inaccuracy incurred in an estimation of the efficiency only from a knowledge of the mass flow and the nacelle internal static pressure was so small as to be masked by the other experimental errors involved. Thus for most of the tests these data only were recorded, occasional traverses being made in order to check the results obtained.

The pressure ratio (total to static) across the tunnel nozzle was maintained, in general, at within $\pm 0{\cdot}2$ per cent of the value corresponding theoretically to a Mach number of 1·400 and, apart from the slow hunt which constituted this error, no fluctuation of the nacelle static pressure was observed, even during surging.

3. *The Intake Mechanism.*—3.1. *General Note.*—For all detailed investigation and in particular for a visual study of the aerodynamic intake mechanism the model E was used with a type II diffuser. This assembly is illustrated in Fig. 7.

Because the incident air is compressed by the intake nacelle some distance upstream of the entry plane the maximum mass flow which can be passed by an intake of the annular variety may be considerably in excess of that comprising the mass in the space volume swept per second by the annulus. However, as it was not practicable to measure accurately the maximum mass flow of an intake, the non-dimensional flow may conveniently be expressed in the form Q/Q_s, where Q_s is the mass of air in the space volume swept per second by the annular intake slot.

Throughout the investigation the actual test readings were computationally so far removed from the final non-dimensional results that considerations of time and power consumption did not permit of an accurate preselection of the points on the final fields. This is the reason for the random distribution of the points on some of the experimental curves and is why the important regions were not always located precisely by observation.

3.2. *With a Laminar Boundary Layer.*—From observations of its behaviour and apparent thickness in striation photographs, the boundary layer on the nacelle of model E appeared to be laminar and the effects of this factor on the intake conditions are demonstrated in Figs. 8, 9. Throughout all the tests a typical λ or bifurcated shock system[3,4,5] was invariably observed to occur on the interaction with the nacelle boundary layer of the substantially normal intake shock. The latter could, moreover, at no time be induced to enter the annulus, even when the maximum mass flow was apparently being passed.

As the mass flow was reduced by throttling, the amount of the supersonic over-expansion, and consequently of the extraneous shock loss in the diffuser, decreased. The intake efficiency thus rose rapidly and, if no shock-wave boundary-layer interaction had been present, would have theoretically reached a maximum value with zero mass flow. However, the interacting boundary layer separated completely from the nacelle surface, and the further upstream the intake shock moved the greater became the relative disturbance created in the entry plane. The efficiency characteristic therefore became flat and exhibited a turning point at or near which, as would happen in an axial flow compressor[6], the system became unstable.

The nature and frequency of the resulting surge were such that fluctuations in the nacelle static pressure could not be detected and measurements of the temporal mean intake efficiency could thus be performed at very small mass flows. However, as this fact is of no practical significance, it appears from Fig. 8 that the useful operating range of model E is defined by $0{\cdot}83 < Q/Q_s < 1{\cdot}05$.

3.3. *With a Turbulent Boundary Layer.*—To produce a thick turbulent boundary layer a ring of 0·010-in. diameter wire was placed around the model nacelle in a position apparent from the fixed extraneous shocks of Fig. 9 and this device seemed approximately to double the boundary-layer thickness. Although not obvious from the striation photographs, the resulting interaction system was found by visual observation to be a λ shock and to be similar to that caused by a laminar boundary layer.

The shock position curves of Fig. 8 refer to the toe of the λ shock and were obtained by measurement from several typical striation photographs. From their relative positions it may be observed that the extent of the interaction disturbance in the entry plane was less with the turbulent than with the laminar boundary layer. This follows from the difference in mass flow at any selected value of s/l, where s is the distance of the shock from the intake plane.

The shift of the efficiency characteristic should, therefore, be ascribed not to the fact that the boundary layer in the second test was turbulent, but to the parasitic loss produced by the wire ring. This effect is precisely analogous to that caused by the nacelle frictional drag of a large model with a turbulent boundary layer and should thus in practice be calculable.

Arising apparently from the increase in the frictional loss, a secondary effect of the change to a turbulent boundary layer was that the useful mass flow range was reduced to approximately $0{\cdot}87 < Q/Q_s < 1{\cdot}00$, the surge point being rather indefinite.

3.4. *The Surge.*—With a laminar nacelle boundary layer the model E was operated in the surged condition at a mass flow, Q/Q_s of 0·571 whilst 162 striation photographs were taken at random during some 2×10^6 surge cycles, each exposure being of about 1×10^{-6} secs. From this batch, of which a few examples are reproduced in Fig. 10, the position of the toe of each λ shock was measured and the resultant data yielded the probability curve of Fig. 8. As each plotted point represents the percentage of the total number of recorded shocks found within a band defined by $s/l \pm 0{\cdot}0125$, this curve is a reasonably accurate statement of the probability of finding the intake shock in any given region during a large number of surge cycles. It may be noted that, in Fig. 9c, the spatial density distribution of the diffused intake shock is as predicted by the probability curve and, as a rough stroboscopic measurement of the surge frequency yielded a result of about 140 c.p.s., this photograph must show the shock distribution as a mean of fewer than 30 cycles.

However, with a periodic motion the probability of finding an object near any point is inversely proportional to the magnitude of its temporal mean velocity, so for any surge cycle each of the extreme intake shock positions must lie on one of the peaked regions of the curve. The rapid decay towards the entry plane, therefore, generalises the previous statement to the effect that the intake shock cannot be easily persuaded to enter the annulus. Mentally condensing the Gaussian contributions to the probability curve, it may then be observed that upstream of the surge point the velocity—or more precisely the rate of change of position on the nacelle—of the intake shock increases with distance from the entry plane. Supported by the flattening at low mass flows of the temporal mean efficiency characteristics and by a visual stroboscopic observation of the surge, this fact suggests that the recurring cycle is qualitatively as illustrated in Fig. 11.

At an s/l of approximately 0·18 the nominal surge point is reached and, the system being then in a state of unstable equilibrium, the intake shock is accelerated away from the entry plane. At an s/l of about 0·28 the shock begins to decelerate and finally comes to rest, but throughout this process the separated boundary layer has so severely restricted the mass flow into the annulus that the flow out through the metering nacelle throttle has appreciably lowered the static pressure in the diffuser. The shock, therefore, is driven downstream with extreme rapidity by the general flow to a point defined approximately by $s/l = 0{\cdot}08$, and, as the diffuser pressure builds up once more, it moves slowly forward to the surge point, the cycle being then repeated indefinitely.

From this description it is evident that the instability and consequent surging of an intake occur as effects of the separation due to shock–boundary-layer interaction on its nacelle. If that separation could be prevented—by boundary-layer suction for instance—the stability problem should, therefore, disappear.

It may be observed from Fig. 10 that the λ-shock structure and the angle and station at which the boundary layer separates from the nacelle surface may vary considerably with time. Of the several interesting details the monstrous λ shock and delayed separation of Fig. 10e are perhaps of most interest.

4. *Interpretation of Results.*—4.1. *General Note.*—From a cursory examination, the design variables of a supersonic annular intake operating at a fixed Mach number would appear to be the Reynolds number, R, based on the nacelle length, the diameter ratio, d_2/d_1, of the annulus and the profile of the nacelle, but a detailed analysis has shown that none of these is, by itself, a convenient parameter for the purposes of correlation. The experimental characteristics of Figs. 12, 13, 14, therefore, should not be considered directly, for each is affected by the operation of at least two independent variables. In the tests with a turbulent boundary-layer rings of 0·010-in. diameter wire were, as before, placed over the nacelles under investigation.

For design purposes, the losses incurred in the use of an intake of the annular or letterbox variety may conveniently be partitioned as follows:—

Inherent losses

(a) Head shock loss.

(b) Intake shock loss.

(c) Nacelle frictional loss.

(d) General diffuser loss.

Parasitic losses

(e) Interaction loss.

(f) Consequent additional diffuser loss.

Although the inherent losses can be estimated with a reasonable degree of certainty, the two parasitic components are difficult to separate. In the subsequent text they will, therefore, be covered by the single term parasitic loss and considered as constituting the difference between the total experimental loss and the sum of its inherent components.

4.2. *The Significant Parameter.*—Should the losses and the design variables be arranged in the table

Loss	a	b	c	d	e, f
Variable					
R			X	X	X
d_2/d_1			X	X	X
Nacelle Profile	X	X			

where X signifies a first order effect, it will be observed that the inviscid (a, b) and viscous (c, d, e, f) losses may completely be separated and a single parameter thus used to represent the scale effect. However, for any given intake the loss components (c), (d) are calculable, so that the only unknown scale effect is that of the variation of the parasitic loss, which must depend substantially on the relative magnitude of the nacelle boundary layer. The most significant parameter, therefore, is considered to be δ/Δ, where

δ the nacelle boundary-layer thickness which, in the absence of interaction, would theoretically occur in the entry plane and

Δ the intake slot width.

Then, should the inherent losses of the model E be estimated as in Appendix II, the diagram of Fig. 15 may be obtained, the effect of the nacelle shapes considered being assumed sufficiently small at a Mach number of 1·4 to permit of the inclusion of the results for all six models. In the theoretical estimate a nacelle frictional drag coefficient of 0·005 was assumed and the general diffuser efficiency was taken to be $\eta = 0{\cdot}95 - 0{\cdot}25\delta/\Delta$ (*see* Appendix II).

4.3. *Extrapolation.*—In spite of the unfortunate grouping of the experimental points the nature of the problem is such that it should be possible to extrapolate the foregoing results for preliminary full-scale design purposes, this fact depending upon the following circumstances.

I. If the problem of the relative magnitude of the nacelle boundary layer be considered in greater detail, it will be found that the parasitic losses incurred on interaction with the intake shock depend mainly on two factors, namely,

(i) the total energy lost within the boundary layer before interaction and (ii) the extent to which the low energy fluid is projected into the main stream on separation.

Moreover, these factors are themselves functions of the following variables

(a) the nacelle frictional temperature rise,

(b) the relative boundary-layer thickness, δ/Δ,

(c) the nature (stability) of the boundary layer,

(d) the aircraft Mach number.

Of these, (d) does not come within the scope of the investigation and (b) has already been considered. For the purposes of extrapolation it is thus desirable that some account be taken of (a) and (c) and this may be done as follows:

II. If the ratio of the parasitic to the nacelle frictional loss be plotted as a function of the relative boundary-layer thickness, as in Fig. 16a, it will be observed to approach a value of about 2·0. Although there is a considerable scattering of the experimental points this is most probably due to a random element in the nature of the separation of the various thin laminar boundary layers, so the result for model A may be taken as lying close to the final curve, the nacelle boundary layer in this case being much nearer the state of automatic transition at the λ-shock base. As the boundary layer on a full-scale nacelle will probably be turbulent with $\delta/\Delta \geqslant 0{\cdot}2$, values of the parasitic loss given by the extrapolated curve of Fig. 16a may be taken as reasonably correct.

III. An examination of the experimental efficiency mass flow characteristics will show that they are all of substantially the same form and that, with a turbulent boundary layer, the surge point will probably occur at a mass flow of or less than approximately $0{\cdot}8Q_{\max}$. Moreover, most of the characteristics become flat at a mass flow of about $0{\cdot}93Q_{\max}$, so the useful working range of a full-scale intake may be taken as $0{\cdot}8 < Q/Q_{\max} < 0{\cdot}93$.

IV. As the ducting or engine system behind a practicable supersonic annular intake must choke it may easily be shown that first order changes in the mass flow will be defined by an equation of the type $Q/Q_s = (1 + \text{const.}\,\eta)^{\gamma/(\gamma-1)}$

Moreover, in the useful efficiency range such a curve will be so nearly straight that the variation of mass flow with intake efficiency may reasonably be taken as linear. In view of the similarity between the various experimental characteristics the variation with maximum mass flow of the maximum intake efficiency may, therefore, be represented as in Fig. 16b, where the significant curve is, of course, that for the turbulent boundary layer.

Therefore, if the above argument prove to be valid, the rules for extrapolations to full-scale intake systems will be as follows:—

(i) The intake considered must have a nacelle of which the profile approximates to a fractional ogive of the family defined by the limiting members 3/6 and 5/10.

(ii) The ratio of the parasitic loss to the nacelle frictional loss should then be obtained from Fig. 16a.

(iii) The maximum mass flow defined by the equation

$$\eta_{max} = 0{\cdot}497 + 0{\cdot}3Q_{max}/Q_s.$$

(iv) The useful working range taken as

$$0{\cdot}8 < Q/Q_{max} < 0{\cdot}93.$$

5. *Boundary Layer Segregation.*—From Fig. 15 it appears that for a small model the parasitic component of the intake loss amounts to a considerable proportion of the whole and extrapolation by the method of section 4.3 above will shew that this is quite general. A device for the substantial reduction of that loss component, therefore, would be of value and for this purpose the use of boundary-layer suction has been suggested.

However, as is shewn by the shock displacement curves of Fig. 8, the suction, if it is to be effective over the useful working range of an intake, must commence not in the entry plane but at a distance upstream from there, equal approximately to three times the width of the intake slot. An attractive possibility is thus that of distributed suction through a porous nacelle surface, but until further work on the subject has been undertaken it may be difficult to estimate the amount of air which must be removed in this way to stabilise a given boundary layer. As a simpler alternative, the process of local boundary-layer segregation is suggested and illustrated in Fig. 17.

Because of practical difficulties associated with manufacture, flexural rigidity and erosion, it was not considered feasible to test such an arrangement on a model of the scale so far investigated experimentally. It should, however, not only be possible but practicable to perform such an investigation in free flight on an intake of the calibre of that considered in section 6.2 below.

6. *Examples of Extrapolation to Full Scale.*—6.1. *High Speed Research Aircraft.*—The example considered below is that of the annular intake of a single-engined aircraft designed to maintain level flight at a Mach number of 1·4 at 50,000 ft. It is assumed that the aircraft nacelle diameter is 48 in., its profile that of a 4/8 fractional ogive and that 100 lb/sec must be aspirated by the engine, the details of the calculation being given in Appendix III.

It appears that an outside annulus diameter of 58·1 in. is required and that, at the design point, the theoretical partition of loss is as follows:—

Component Loss	Without segregation		With segregation	
	Value	Fraction of total	Value	Fraction of total
Head shock	1·5	10	1·5	12
Intake shock	0·9	6	0·9	7
Nacelle frictional	2·7	18	2·7	22
General diffuser	3·3	21	3·3	27
Parasitic	7·0	45	4·0	32
Total	15·4 per cent	100 per cent	12·4 per cent	100 per cent

With the addition of a $\frac{1}{4}$-in. thick segregation ring of approximate internal diameter 51·5 in. it is assumed that the parasitic loss will be reduced to the value of a component representing the total drag of the ring. The efficiency should then increase by some 3 per cent and, from Fig. 16b, it may be observed that the outside annulus diameter can be reduced to 57·4 in.

On such an aircraft it thus appears that the efficiency of a plain annular intake might be about 85 per cent and that, by the addition of a boundary-layer segregation ring, this might be raised to 88 per cent whilst the intake area is slightly reduced. Moreover, of the remaining 12 per cent loss all need not be considered unfortunate, for it should be noted that the nacelle frictional loss, if not debited to the intake, would otherwise appear as part of the aircraft drag.

With a safe working range of 86 to 100 lb/sec the swept mass flow of the intake at its design point should be

without segregation = 92·3 lb/sec

or

with segregation = 85·1 lb/sec

6.2. *Rocket-propelled Intake Model.*—Also considered in Appendix III is the performance of such an intake model as might be intended for confirmatory tests at a Mach number of 1·4 at sea level with a Reynolds number of about 8×10^6. The 5-in. diameter nacelle is assumed to have the profile of 4/8 fractional ogive, the outside annulus diameter to be 6 in. and the unit might, for example, be rocket propelled.

The segregation ring envisaged for this model would be 0·025 in. thick with an approximate internal diameter of 5·4 in. On its addition both the efficiency and mass flow might be expected to increase and, the swept mass flow being 7·2 lb/sec, the overall effects are theoretically as follows:

Performance without ring

Intake efficiency = 80 per cent

Useful range = 5·8 to 6·8 lb/sec

Performance with ring added

Intake efficiency = 85 per cent

Useful range = 6·8 to 7·9 lb/sec

The detailed theoretical loss analysis is:—

Component Loss	Without segregation		With segregation	
	Value	Fraction of total	Value	Fraction of total
Head shock	1·5	7	1·5	10
Intake shock	0·9	4	0·9	6
Nacelle frictional	3·8	19	3·6	24
General diffuser	4·8	24	4·8	31
Parasitic	9·2	46	4·4	29
Total	20·2 per cent	100 per cent	15·2 per cent	100 per cent

7. *Operational Variables.*—7.1. *Mach Number.*—As the shock losses of an annular intake of the type considered should increase rapidly with Mach number and become prohibitive at about 1·6 such a system would be of little use for cruising speeds of much over 1000 m.p.h. in the stratosphere.

Moreover, owing to the formation at various stations on the nacelle of one or more extraneous λ shocks, the parasitic intake loss may be relatively high at large subsonic Mach numbers, but as sonic speed is reached this effect should decrease and in supersonic flight should vary but little with Mach number in the range considered.

With a specified intake, changes in the nacelle frictional and general diffuser loss components may, of course, be considered as Reynolds number effects.

7.2. *Pitch and Yaw.*—Although, in so far as complete annular intakes are concerned, pitch and yaw angles need not be considered separately, only the former are of much significance. The worst design condition which may reasonably be considered is thus that which would be attained by a supersonic aircraft in a 6*g* turn at sonic speed at 50,000 ft, when the angle of incidence of the intake axis should not exceed 20 deg. However, even at such an incidence the performance of a typical annular entry might not seriously be affected, for as the head angle of a 4/8 fractional ogive is 43 deg such a profile would still provide some expansion around its worst side.

The consequent axial asymmetry in the intake mass flow distribution will, therefore, be due not so much to variations in the rate of growth of the nacelle boundary layer as to the peripheral variation of the inviscid Mach number in the entry plane. However, as changes in the local mass rate of flow should amount only to a few per cent of the spatial mean value they should have no serious effect on the aerodynamic stability of the engine compressor.

8. *Conclusion.*—The stability of the annular type of air intake has been considered in detail at a flight Mach number of 1·4 and it has been shewn that an acceptable mass flow range might safely be obtained in practice. The experimental results were obtained at Reynolds numbers around $1{\cdot}5 \times 10^6$ and an extrapolation suggests that a typical full-scale aircraft intake would have an overall isentropic efficiency of about 85 per cent.

Boundary-layer suction on the nacelle surface is apparently a possibility for improving both the stability and the efficiency of the system, but it has not been considered in this note. As an alternative a local segregation of the boundary layer is suggested, and a rough estimation shews that the use of a thin ring for this purpose (*see* Fig. 17) might raise the typical efficiency by some 2 or 3 per cent.

9. *Recommendation.*—As the Reynolds numbers of the annular intake models so far tested have not exceeded $1{\cdot}8 \times 10^6$, the aforementioned full-scale performance figures were derived entirely by extrapolation. Therefore, it is suggested that before these results can be accepted at least one confirmatory test should be performed at a Reynolds number greater than 10^7.

REFERENCES

No.	*Author*	*Title, etc.*
1	G. H. Lean	On the Flow Phenomena at Supersonic Speed in the Neighbourhood of the Entry of a Propulsive Duct. A.R.C. 11,868, 1945. (To be published).
2	E. L. Place and A. G. Smith ..	Supersonic Diffusion in the Presence of a Boundary Layer. Power Jets Ltd. (R. & D.). Memo. No. 1071, February, 1945. (Unpublished).
3	A. Fage and R. F. Sargent	Shock-wave and Boundary-layer Phenomena near a Flat Surface. *Proc. Roy. Soc.*, Series A; Vol. 190, p.1; June, 1947.
4	J. Ackeret, F. Feldmann and N. Rott ..	Untersuchungen an Verdichtungsstössen und Grenzshichten in schnell-bewegten Gasen. *E.T.H. Aero. Ber.* 10; 1946.
5	H. W. Liepmann	The Interaction Between Boundary Layer and Shock-waves in Transonic Flow. *J. Aero. Sci.* Vol. 13, No. 11; December, 1946.
6	A. R. Howell	The Present Basis of Axial-flow Compressor Design. Part II. R.A.E. Report E. 3961. December, 1942.
7	G. I. Taylor and J. W. Maccoll ..	The Air Pressure on a Cone moving at High Speeds. *Proc. Roy. Soc.*, Series A; Vol. 139; February, 1933.

NOMENCLATURE

p	Absolute pressure
p_{tot}	Total pressure
T	Absolute temperature
T_{tot}	Total temperature
ν	Kinematic viscosity
ρ	Density
γ	Isentropic exponent
Q	Mass rate of flow
Q_s	Mass in the space volume swept per second
Q_{max}	Maximum mass rate of flow
l	Nacelle length
s	Station on nacelle measured axially from the entry plane
d_1	Internal diameter of annulus
d_2	External diameter of annulus
A	Annular slot width
δ	Theoretical boundary-layer displacement thickness in entry plane
η	Intake efficiency
M	Mach number
R	Reynolds number

N.B. The intake efficiency is given by

$$\eta = \frac{(p_{tot} \text{ after diffusion/atmospheric pressure})^{(\gamma-1)/\gamma} - 1}{\frac{\gamma-1}{2}\,(\text{Aircraft Mach number})^2}$$

APPENDIX II

Theoretical Loss Analysis for Model E

Head Shock Loss.—The loss in total pressure caused by the head shock is found by assuming that, for a 4/8 fractional ogive, the shock intensity near the profile is the same as that which would occur with a cone of the same apex angle, namely 43·3 deg. Then it follows from the established theory[7] that the efficiency of the head shock is 98·5 per cent.

The free-stream conditions assumed upstream of the head shock are $p = 14{\cdot}7$ lb/sq in. abs., $p_{tot} = 46{\cdot}78$ lb/sq in. abs., $T = 332{\cdot}5$ deg K, $T_{tot} = 462{\cdot}8$ deg K, so that the useful temperature rise in a perfect intake would be 130·3 deg C.

Intake Shock Loss.—Because of the head-shock loss it is assumed that the air, if expanded isentropically around the nacelle and fuselage until its streamlines were parallel to those of the free stream, would attain a Mach number not of 1·4 but that corresponding to

$$T_{tot}/T = 1+0{\cdot}985\ \frac{130{\cdot}3}{332{\cdot}5} = 1{\cdot}386$$

This Mach number is 1·384.

However, at the shoulder of a 4/8 fractional ogive the surface is inclined at 7·2 deg from the axial direction so that, with the assumption that the last few degrees of the 22 deg expansion is approximately two-dimensional, the Mach number just upstream of this point would appear to be 1·108. The efficiency of the substantially normal intake shock is thus 99·1 per cent and the combined shock efficiency 97·6 per cent whilst the Mach number in the entry plane is 0·906.

Nacelle Frictional Loss.—A detailed calculation will then show that the exact theoretical Reynolds number in the intake plane is nearly the same as that derived from the assumption of free-stream conditions and an effective surface length of l, the nacelle axial length. Using the latter value we thus have, with a viscosity of $2{\cdot}04 \times 10^{-4}$ sq ft/sec, $R = 1{\cdot}302 \times 10^6$. But the length of the nacelle surface arc is 1·966 in. so that, with a laminar boundary layer,

$$\delta = \frac{5{\cdot}5x}{\sqrt{R}} = 0{\cdot}00948 \text{ in. and } \frac{\delta}{\Delta} = 0{\cdot}0551.$$

The conditions just before the intake shock are $p = 21{\cdot}61$ lb/sq in. abs. and $T = 371{\cdot}6$ deg K and for a rough estimate of the frictional drag it is assumed that, together with the local velocity of 1405 ft/sec, these occur at all points on the nacelle. With a surface area of 3·03 sq in. and a drag coefficient of 0·005 the frictional drag thus appears to be 0·281 lb.

Accordingly, the drag power $= (0{\cdot}281 \times 1405)/1400 = 0{\cdot}282$ C.H.U./sec.

Now the intake area is 0·6227 sq in. and at 1405 ft/sec the local density is 0·002708 slugs/cu ft so that, neglecting the effect of the boundary layer, the mass flow is 0·530 lb/sec. As this value is about 1·1 times the swept mass it appears that the model is under consideration at maximum efficiency and near its surge point.

Then, expressing the frictional loss as a rise in temperature of the total mass of air aspirated, the frictional temperature rise is

$$\frac{0{\cdot}282}{0{\cdot}530 \times 0{\cdot}238} = 2{\cdot}24 \text{ deg C.}$$

Therefore, the corresponding efficiency increment is −1·72 per cent, whence, neglecting parasitic losses, the intake efficiency defining the mean total conditions in the entry plane is 95·9 per cent.

General Diffuser Loss.—With the efficiency of 95·9 per cent the mean conditions in the entry plane are $M = 0{\cdot}906$ and $P_{tot} = 44{\cdot}9$ lb/sq in. abs. As the area ratio of the diffuser is 2·84, isentropic diffusion would therefore produce a final Mach number of 0·208 and a pressure of 43·6/sq in. abs.

Now the diffuser efficiency may be defined by

$$\eta = 1 - \left(\frac{p_{tot1} - p_{tot2}}{p_2 - p_1}\right)$$

where the suffices 1 and 2 represent the initial and final conditions respectively, and it is taken to be

$$\eta = 0{\cdot}95 - 0{\cdot}25\,\delta/\Delta$$

In the system under consideration the diffuser efficiency, therefore, is 93·6 per cent and the consequent total pressure loss 1·10 lb/sq in.

Thus, neglecting the parasitic losses, the total pressure in the metering nacelle after diffusion is 43·8 lb/sq in. abs. and the overall intake efficiency 93·6 per cent.

The chart of Fig. 15 may then be obtained by a repetition of the above process for several arbitrary values of d_2.

APPENDIX III

Examples of Extrapolation

It may be observed that in both examples parts of the calculation must consist of a process of successive approximation. In such circumstances only the values for the final stage of each of these processes is given.

Example I. Research Aircraft.

The pertinent atmospheric conditions are:—

$p = 1{\cdot}682$ lb/sq in. abs. and $T = 216{\cdot}6$ deg K.

whence, $\rho = 0{\cdot}000362$ slugs/cu ft and $\nu = 5{\cdot}65 \times 10^{-4}$ sq ft/sec.

Other design conditions are

$M = 1{\cdot}40$, $Q = 100$ lb/sec, $d_1 = 48{\cdot}0$ in. and, with a 4/8 fractional ogive as the nacelle profile, the Reynolds number is $18{\cdot}7 \times 10^6$.

The design point is taken as $Q/Q_{max} = 0{\cdot}93$ with an assumed value for Q_{max}/Q_s of 1·003 so that $d_2 = 59{\cdot}6$ in. and with a turbulent boundary layer $\delta = \dfrac{0{\cdot}375x}{1/5} = 1{\cdot}222$ in. Then, by the method of Appendix II, the combined shock efficiency is 97·6 per cent, the frictional temperature rise 2·28 deg C and the resultant efficiency in the entry plane 94·9 per cent.

As the intake is envisaged for use with a high-speed axial-flow compressor its efficiency may be somewhat improved by the avoidance of unnecessary diffusion and the Mach number in the final reference plane is accordingly assumed to be 0·3. Thus, with entry plane conditions of $M = 0{\cdot}906$ and $p_{tot} = 5{\cdot}08$ lb/sq in. abs., the diffuser pressure loss is 0·164 lb/sq in. and the overall intake efficiency, parasitic losses excluded, 91·6 per cent.

But δ/Δ is 0·211. Thus, assuming that the parasitic loss is 2·6 times the nacelle frictional loss, as in Fig. 16a, the application of this factor directly to the pertinent efficiency increment will yield an overall intake efficiency of 84·6 per cent.

In accordance with Fig. 16b, the external annulus diameter can thus be reduced to 58·1 in. and, the performance being unaffected, the swept mass to 93·2 lb/sec.

With the addition of a boundary-layer segregation ring the parasitic loss may then be taken only to be the loss associated with the drag of the ring and this drag is assumed to consist of

(i) a frictional component defined by the action on the surface area of the ring of a coefficient of magnitude 0·005

and (ii) a form component which may be estimated by the assumption of the operation of the coefficient 0·55 on the ring frontal area.

The ring internal diameter, thickness and chord being respectively 51·5, 0·25 and 15·0 in., the drag is thus 99 lb and the parasitic efficiency increment —4·0 per cent.

The overall intake efficiency is thus 87·6 per cent and the external annulus diameter may be reduced to 57·4 in. so that the swept mass is 85·1 lb/sec.

Example II. Large-scale Model.

The nacelle profile is again taken to be that of a 4/8 fractional ogive but this time the annulus internal and external diameters are respectively specified as 5·0 and 6·0 in. At sea-level the atmospheric conditions may be taken as $p = 14{\cdot}7$ lb/sq in. abs. and $T = 288$ deg K so that, with a Mach number of 1·40, the swept mass is 7·2 lb/sec and the Reynolds number $8{\cdot}04 \times 10^6$.

With a turbulent boundary layer δ/Δ is therefore 0·302 and the design point will be taken as $Q/Q_{\max} = 0{\cdot}93$ at $Q_{\max}/Q_s = 1{\cdot}03$, that is, as 6·72 lb/sec. Therefore, by the method of Appendix II, the frictional efficiency increment is —3·8 per cent and so, assuming no parasitic loss, the mean entry plane efficiency is 93·8 per cent.

Accordingly the entry plane conditions are $M = 0{\cdot}906$ and $p_{\text{tot}} = 44{\cdot}0$ lb/sq in. abs. so that, if the diffusion were continued until an unobstructed 6 in. diameter duct is attained, the final isentropic Mach number would be 0·179. Thus, neglecting the parasitic loss, the diffuser pressure loss of 2·13 lb/sq in. yields an overall intake efficiency of 89·0 per cent.

Therefore, assuming from Fig. 16 a the factor of 2·4, the parasitic efficiency increment is 9·2 per cent and the final value for the intake efficiency 79·8 per cent.

The diameter, thickness and chord of a segregation ring suitable for the model are respectively 5·4, 0·025 and 1·5 in. and, with $Q_{\max}/Q_s = 1{\cdot}10$ the mass flow at design point would be 7·18 lb/sec.

As the diffuser pressure loss will be substantially unaffected but the nacelle frictional efficiency increment changed by 0·2 per cent the new value for the efficiency of the intake without parasitic effects is 89·2 per cent.

Then, if the ring drag be estimated as in the previous example, the parasitic efficiency increment will be found to be 4·4 per cent so that the overall efficiency of the intake with the ring is 84·8 per cent.

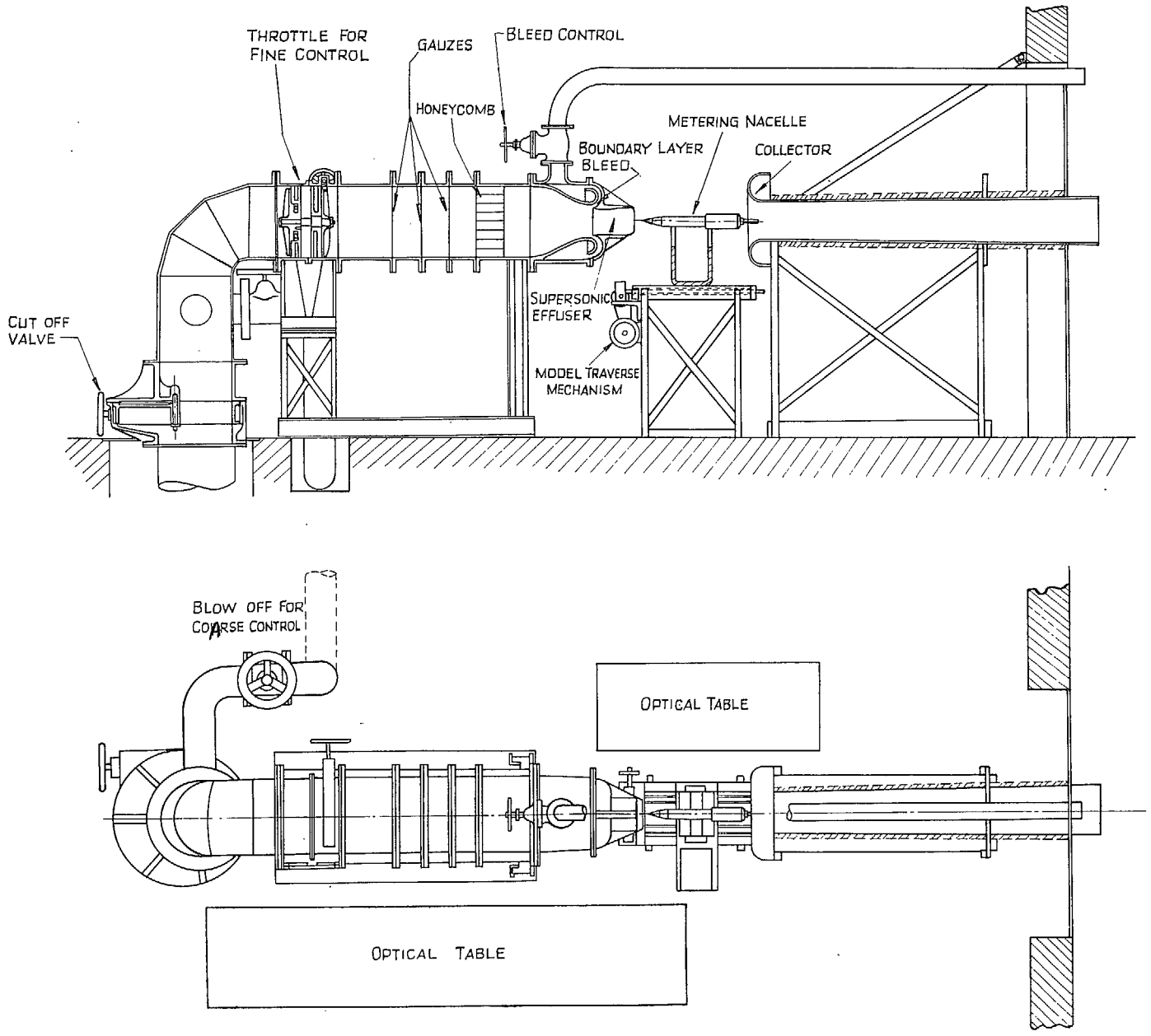

FIG. 1. General arrangement of tunnel.

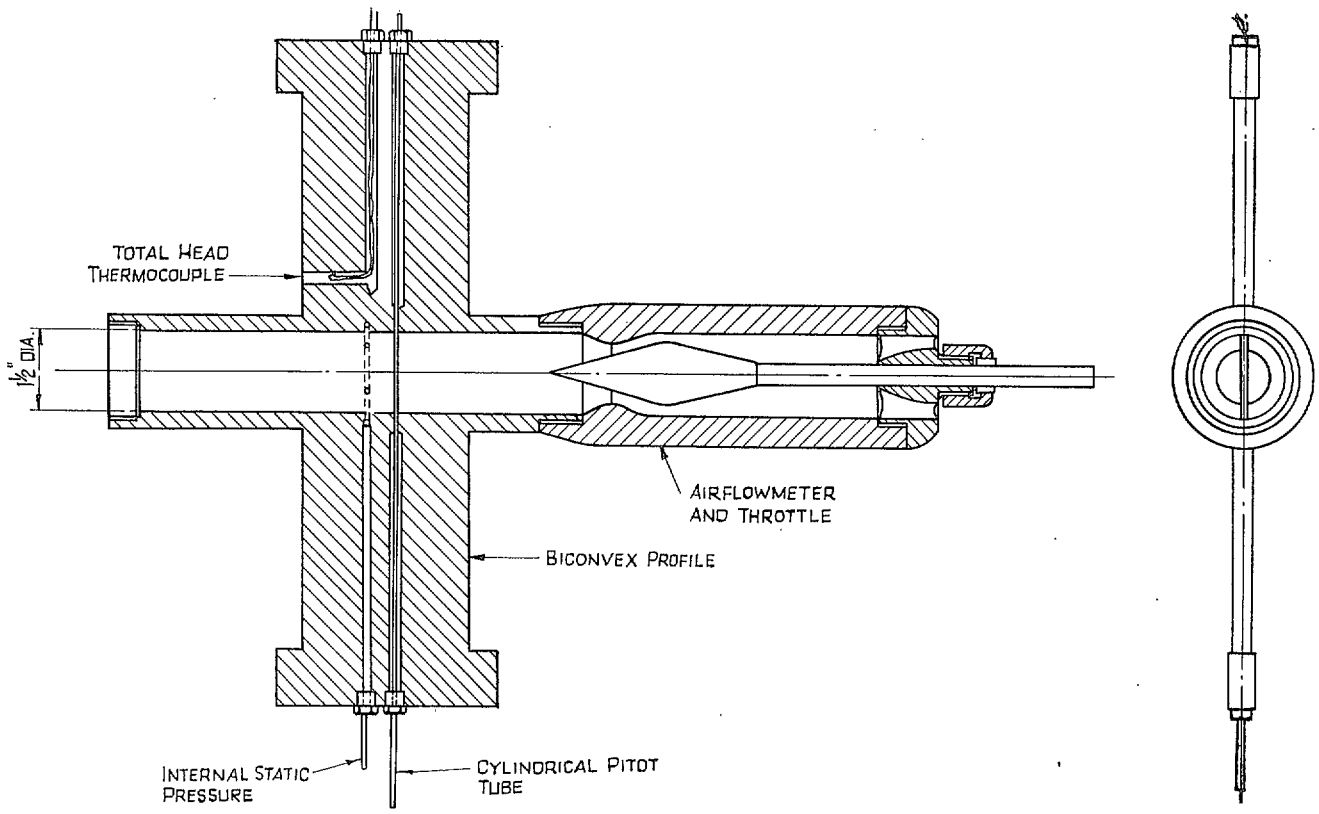

FIG. 2. The metering nacelle.

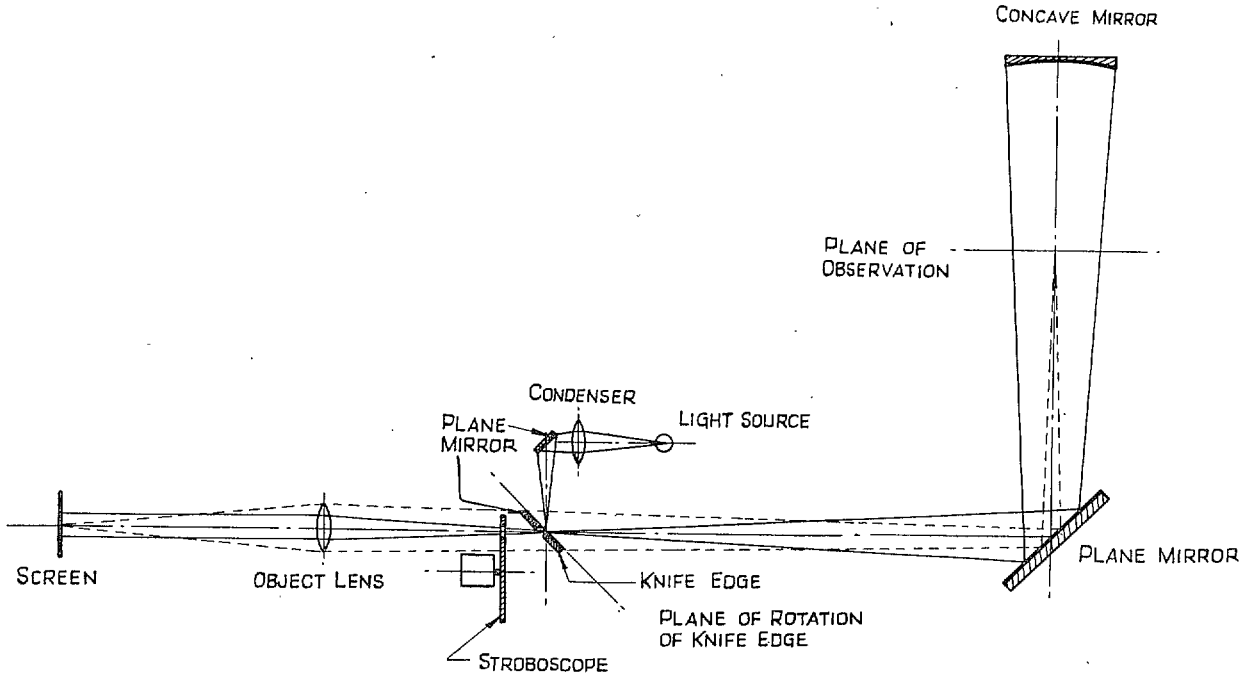

FIG. 3. The striation system.

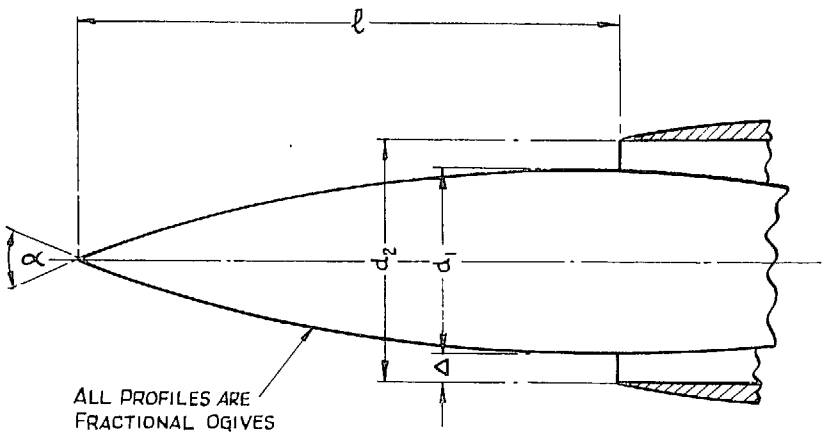

MODEL	PROFILE	d_1 in.	d_2 in.	ℓ in.	α °	R $\times 10^{-6}$	δ/Δ
A	4/8	1·363	1·495	2·79	43·3	1·810	0 1759
B	4/8	1·190	1 495	2·56	43·3	1·581	0·0600
C	4/8	1·136	1 495	2·26	43·3	1·509	0·0582
D	3/6	1·051	1·354	1·74	50·2	1·196	0·0606
E	4/8	0·980	1·324	1·90	43·3	1·302	0·0551
F	5/10	0·948	1·278	2·07	38 6	1·417	0·0593

FIG. 4. Model details,

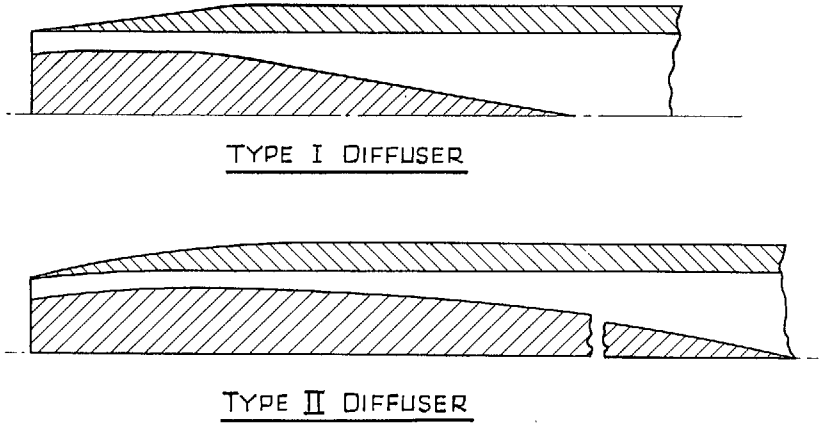

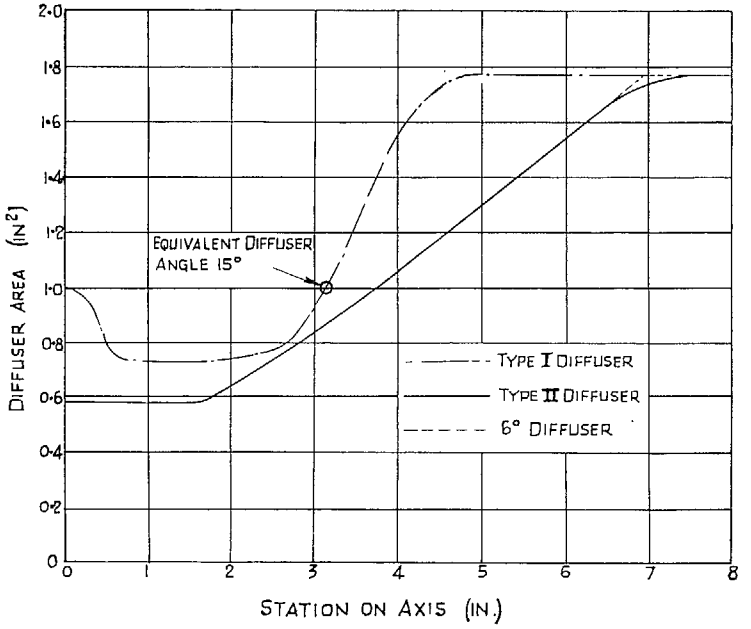

FIG. 5. Diffuser details,

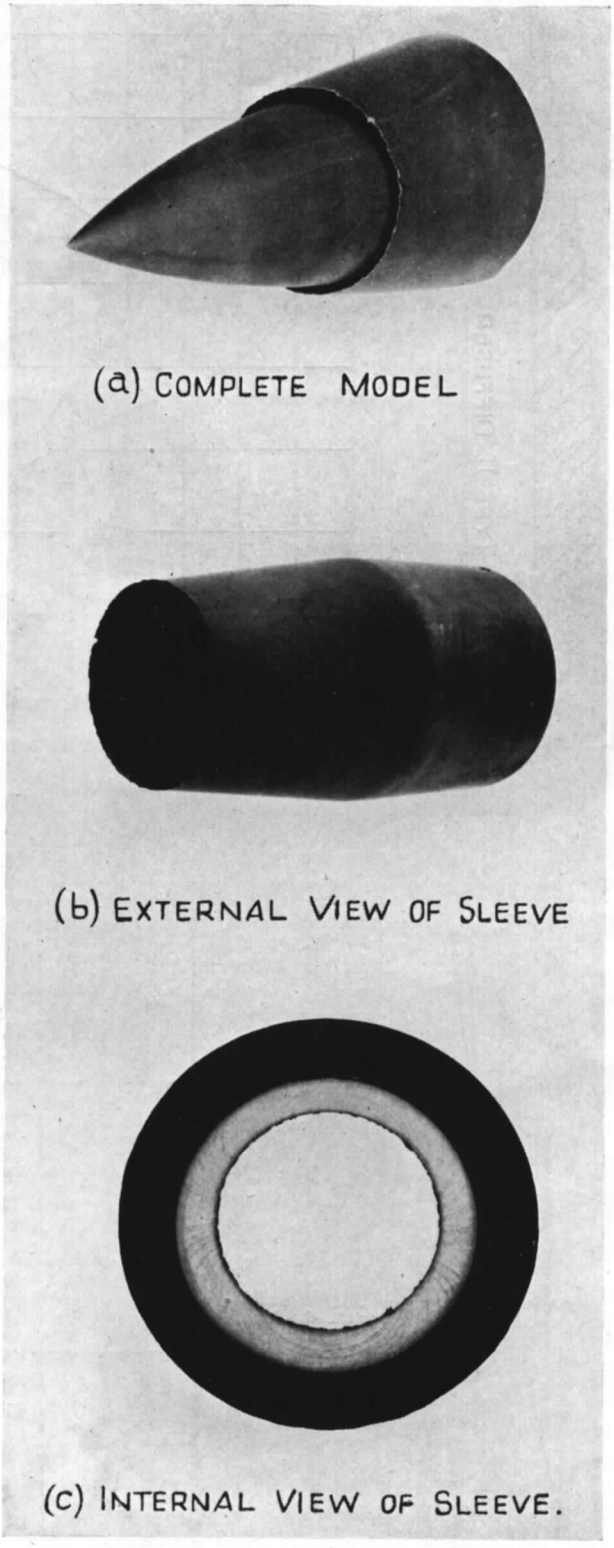

FIG. 6. Severe erosion of model A.

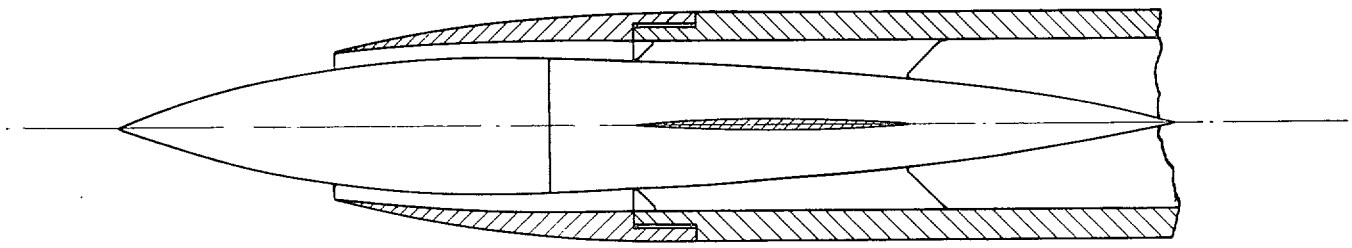

FIG. 7. Model E with type II diffuser.

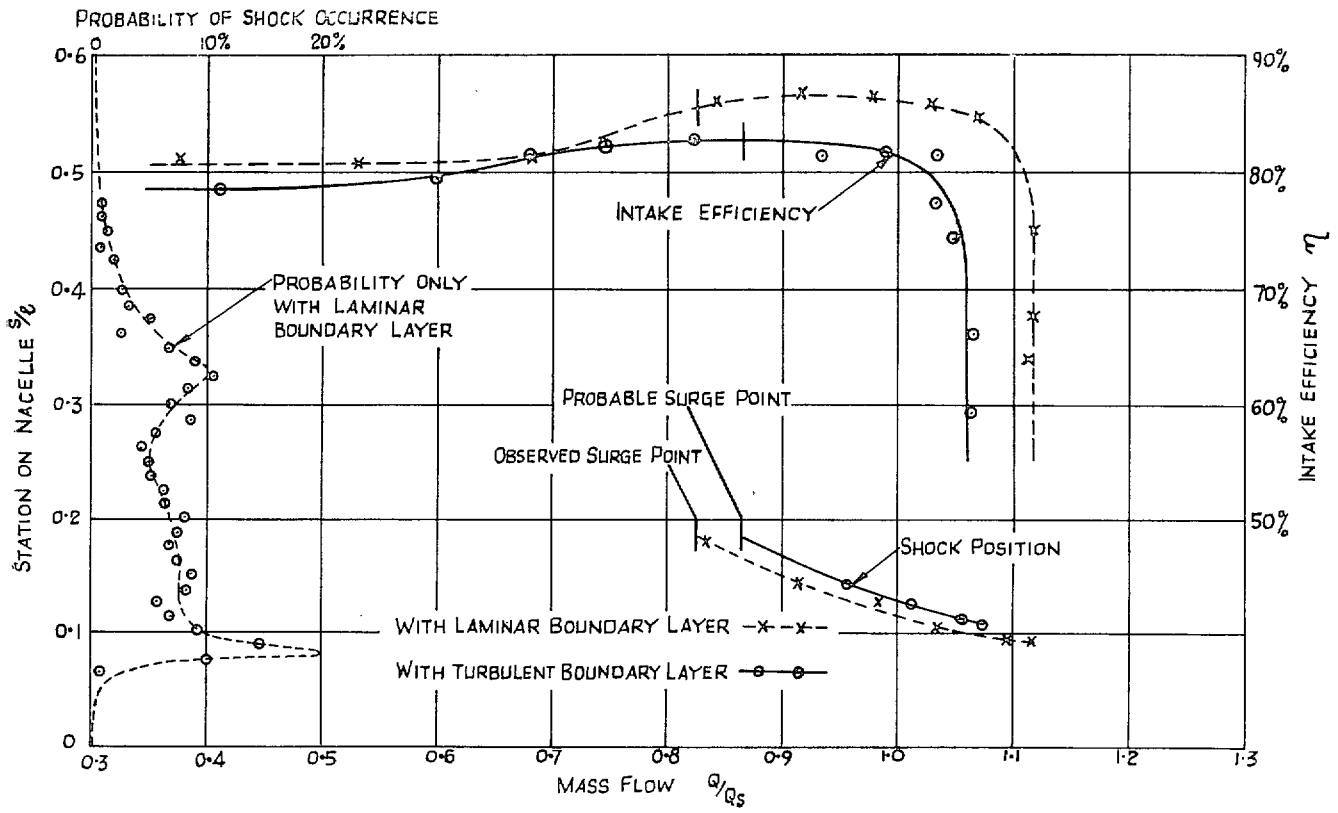

FIG. 8. Intake shock position.

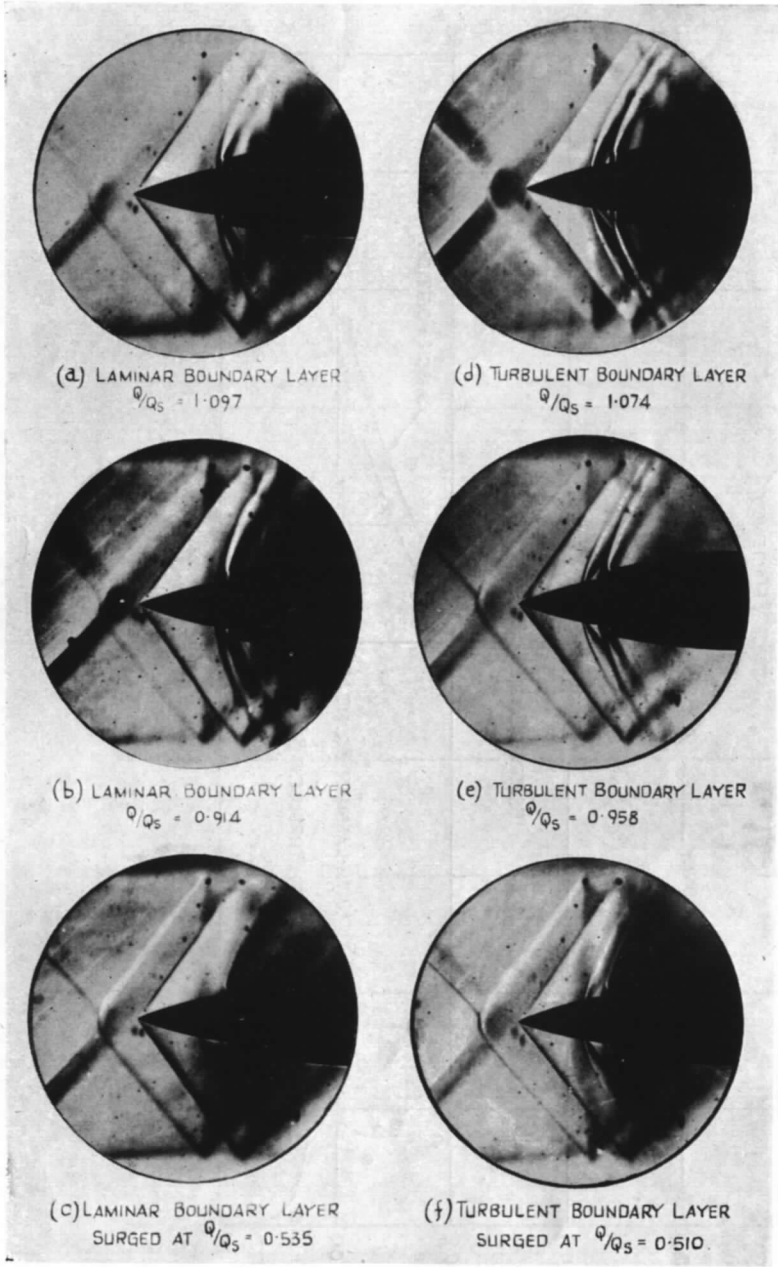

FIG. 9. The intake mechanism (exposures—0·2 sec).

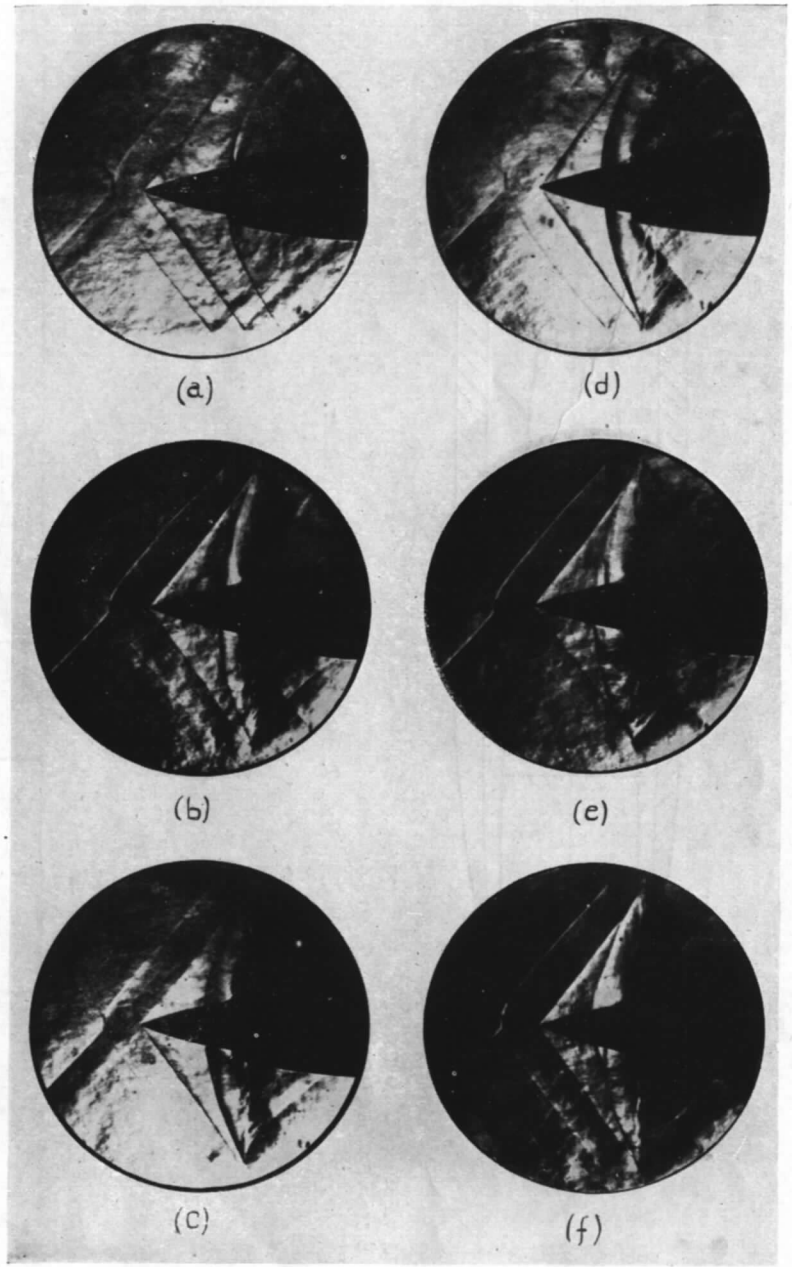

FIG. 10. The surge (exposures—1×10^{-6} sec).

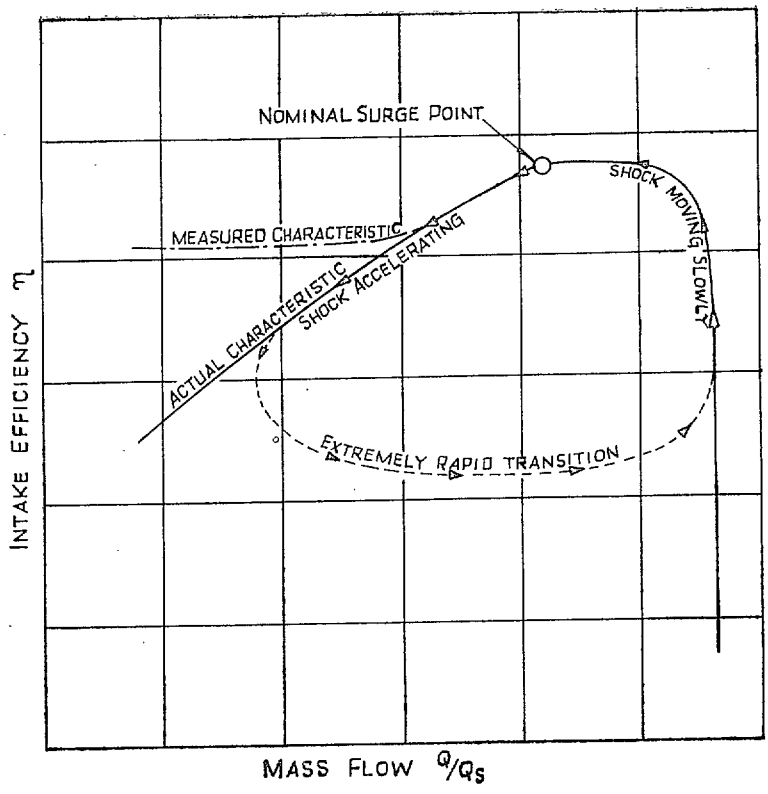

FIG. 11. Probable surge cycle.

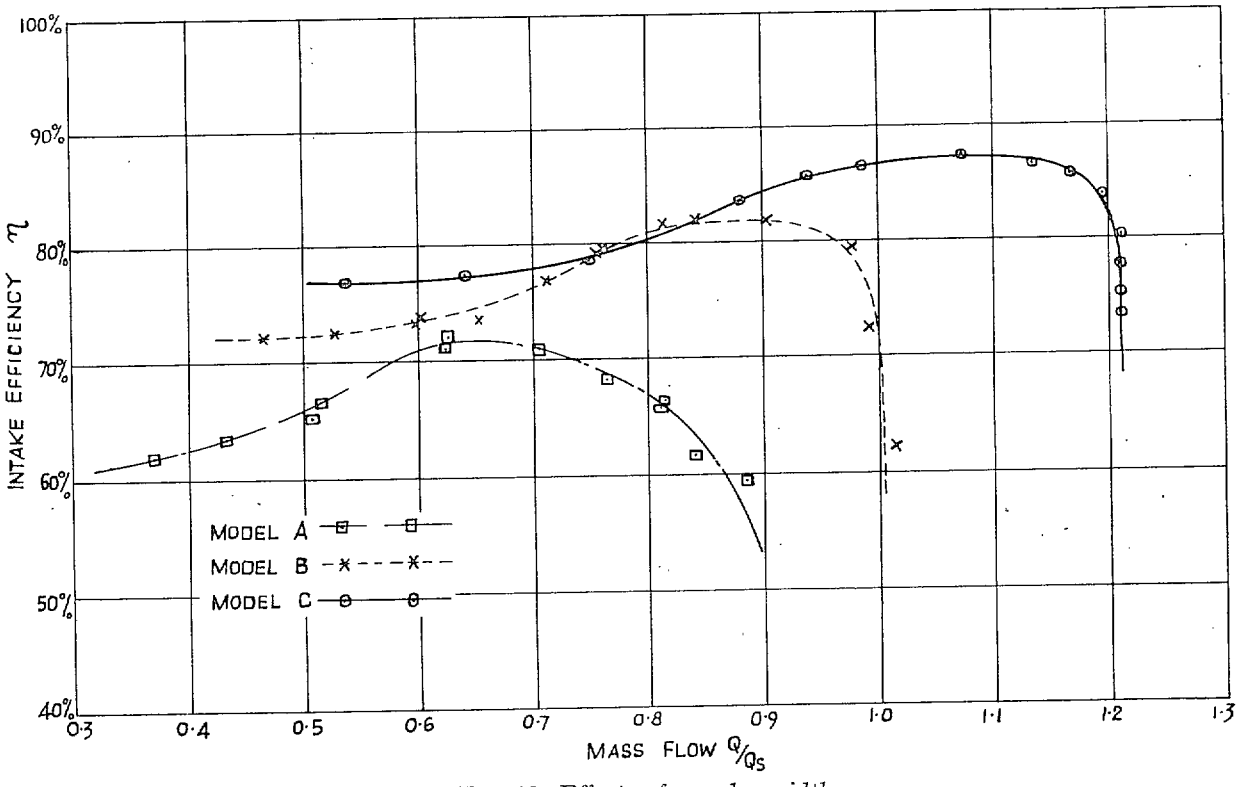

FIG. 12. Effects of annulus width.

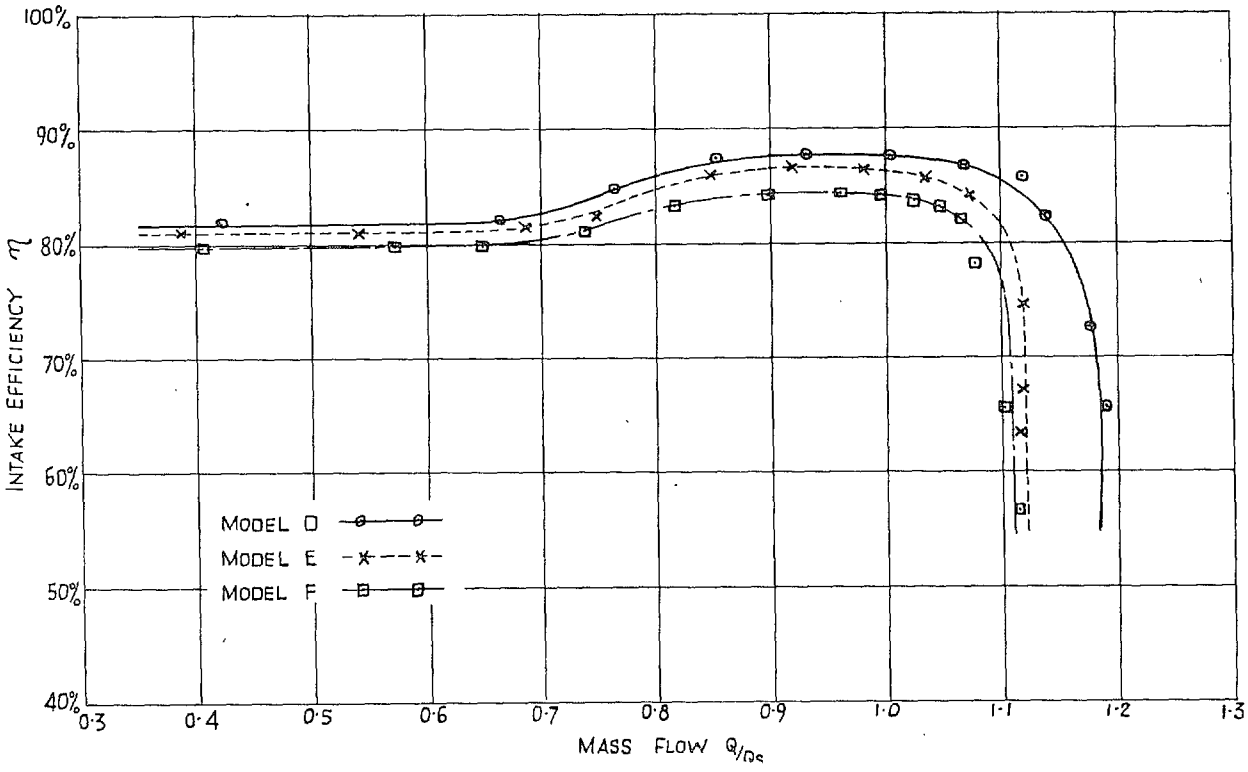

FIG. 13. Effects of nacelle profile.

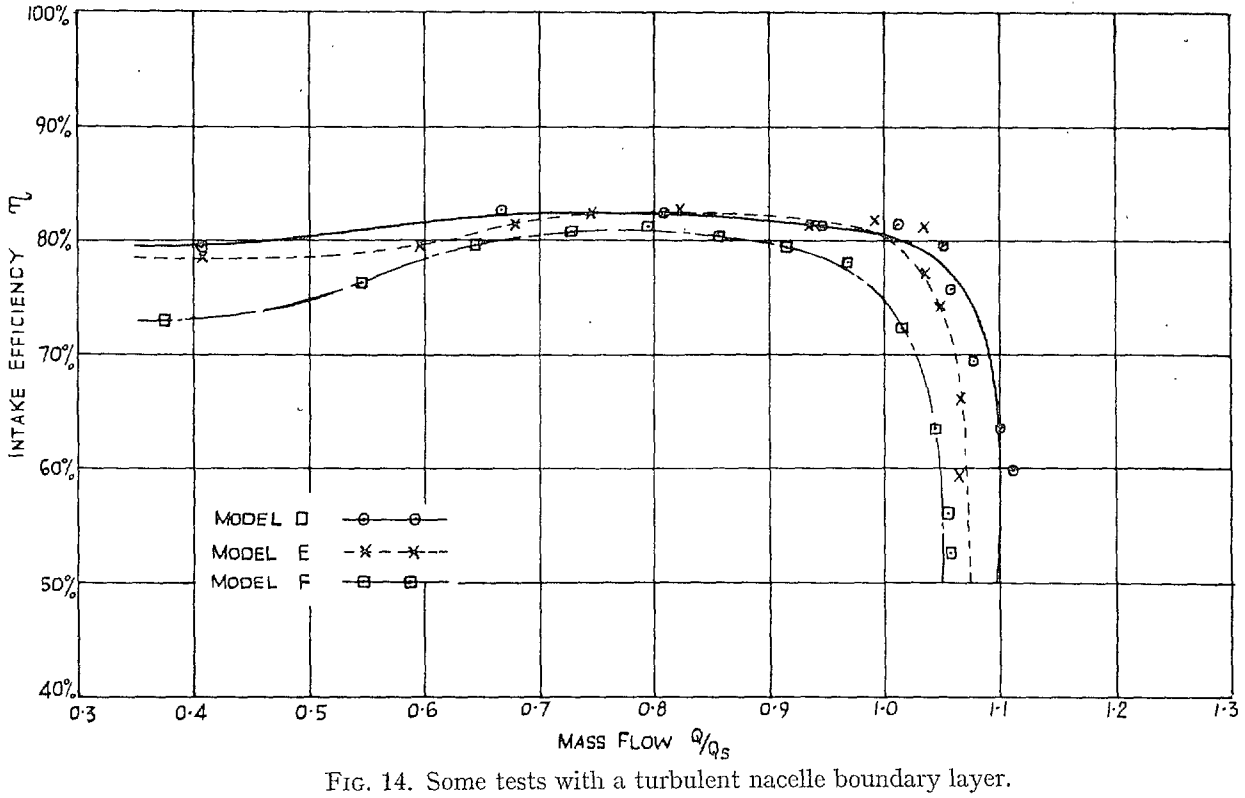

FIG. 14. Some tests with a turbulent nacelle boundary layer.

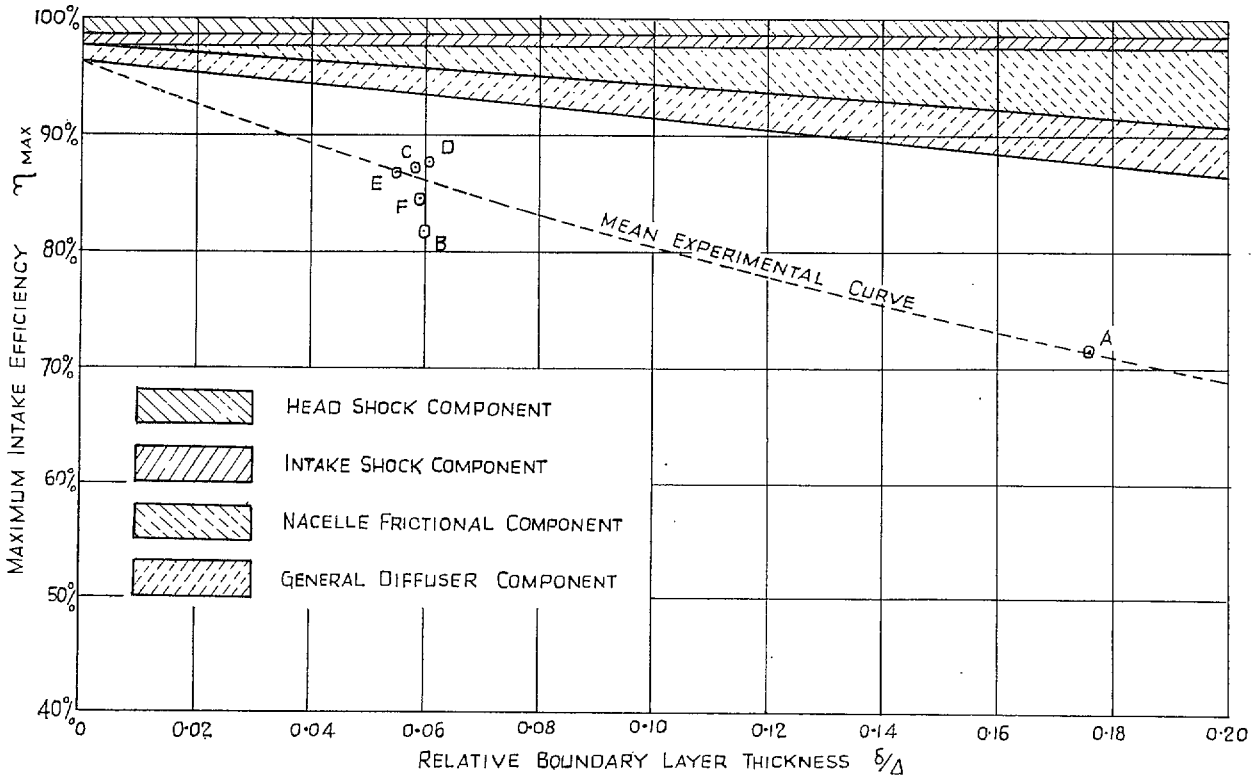

FIG. 15. Correlation of results.

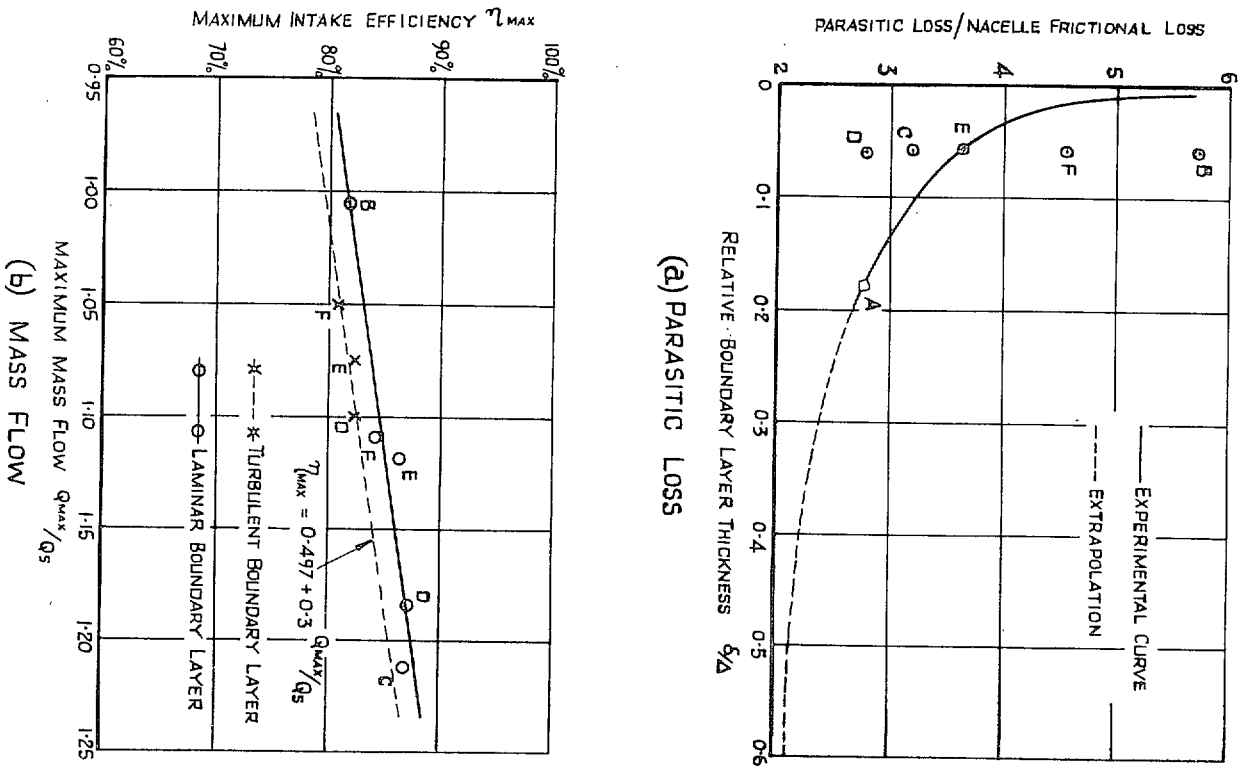

FIG. 16. Extrapolation of results.

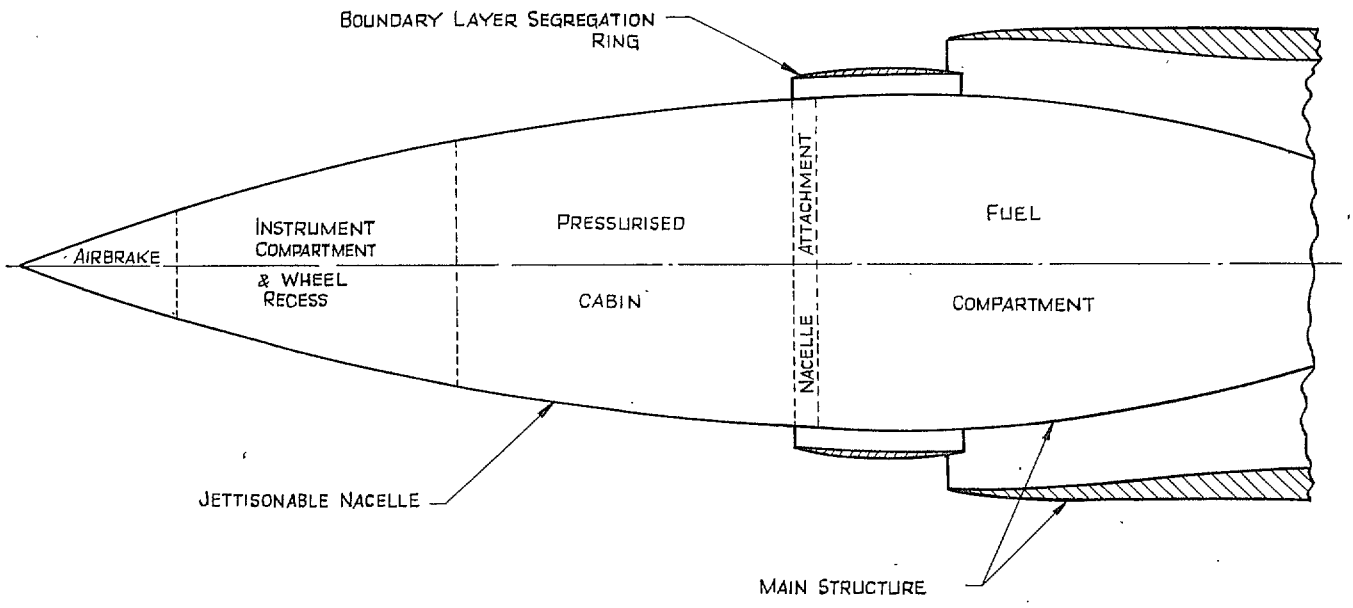

FIG. 17. Typical aircraft intake with boundary-layer segregation.

Ps 13029. Wt. 15/680. K9. 7/51. (H.P.W.—34369). Gp. 1008.

PRINTED IN GREAT BRITAIN

Publications of the Aeronautical Research Council

ANNUAL TECHNICAL REPORTS OF THE AERONAUTICAL RESEARCH COUNCIL (BOUND VOLUMES)

1934–35 Vol. I. Aerodynamics. *Out of Print.*
Vol. II. Seaplanes, Structures, Engines, Materials, etc. 40*s.* (40*s.* 8*d.*)

1935–36 Vol. I. Aerodynamics. 30*s.* (30*s.* 7*d.*)
Vol. II. Structures, Flutter, Engines, Seaplanes, etc. 30*s.* (30*s.* 7*d.*)

1936 Vol. I. Aerodynamics General, Performance, Airscrews, Flutter and Spinning. 40*s.* (40*s.* 9*d.*)
Vol. II. Stability and Control, Structures, Seaplanes, Engines, etc. 50*s.* (50*s.* 10*d.*)

1937 Vol. I. Aerodynamics General, Performance, Airscrews, Flutter and Spinning. 40*s.* (40*s.* 10*d.*)
Vol. II. Stability and Control, Structures, Seaplanes, Engines, etc. 60*s.* (61*s.*)

1938 Vol. I. Aerodynamics General, Performance, Airscrews. 50*s.* (51*s.*)
Vol. II. Stability and Control, Flutter, Structures, Seaplanes, Wind Tunnels, Materials. 30*s.* (30*s.* 9*d.*)

1939 Vol. I. Aerodynamics General, Performance, Airscrews, Engines. 50*s.* (50*s.* 11*d.*)
Vol. II. Stability and Control, Flutter and Vibration, Instruments, Structures, Seaplanes, etc. 63*s.* (64*s.* 2*d.*)

1940 Aero and Hydrodynamics, Aerofoils, Airscrews, Engines, Flutter, Icing, Stability and Control, Structures, and a miscellaneous section. 50*s.* (51*s.*)

Certain other reports proper to the 1940 *volume will subsequently be included in a separate volume.*

ANNUAL REPORTS OF THE AERONAUTICAL RESEARCH COUNCIL—

1933–34 1*s.* 6*d.* (1*s.* 8*d.*)
1934–35 1*s.* 6*d.* (1*s.* 8*d.*)
April 1, 1935 to December 31, 1936. 4*s.* (4*s.* 4*d.*)
1937 2*s.* (2*s.* 2*d.*)
1938 1*s.* 6*d.* (1*s.* 8*d.*)
1939–48 3*s.* (3*s.* 2*d.*)

INDEX TO ALL REPORTS AND MEMORANDA PUBLISHED IN THE ANNUAL TECHNICAL REPORTS, AND SEPARATELY—

April, 1950 R. & M. No. 2600. 2*s.* 6*d.* (2*s.* 7½*d.*)

INDEXES TO THE TECHNICAL REPORTS OF THE AERONAUTICAL RESEARCH COUNCIL—

December 1, 1936—June 30, 1939 R. & M. No. 1850. 1*s.* 3*d.* (1*s.* 4½*d.*)
July 1, 1939—June 30, 1945. R. & M. No. 1950. 1*s.* (1*s.* 1½*d.*)
July 1, 1945—June 30, 1946. R. & M. No. 2050. 1*s.* (1*s.* 1½*d.*)
July 1, 1946—December 31, 1946. R. & M. No. 2150. 1*s.* 3*d.* (1*s.* 4½*d.*)
January 1, 1947—June 30, 1947. R. & M. No. 2250. 1*s.* 3*d.* (1*s.* 4½*d.*)

Prices in brackets include postage.

Obtainable from

HER MAJESTY'S STATIONERY OFFICE

York House, Kingsway, LONDON, W.C.2 429 Oxford Street, LONDON, W.1
P.O. Box 569, LONDON, S.E.1
13a Castle Street, EDINBURGH, 2 1 St. Andrew's Crescent, CARDIFF
39 King Street, MANCHESTER, 2 Tower Lane, BRISTOL, 1
2 Edmund Street, BIRMINGHAM, 3 80 Chichester Street, BELFAST

or through any bookseller